Odd-even absorption and Coulomb-exchange effects in the $^3He + ^4He$ and $^3H + ^4He$ systems*

J. A. Koepke, Ronald E. Brown, Y. C. Tang, and D. R. Thompson
School of Physics, University of Minnesota, Minneapolis, Minnesota 55455

(Received 2 July 1973)

Differential cross sections for $^3He + ^4He$ elastic scattering are calculated at c.m. energies up to 44.5 MeV using the one-channel resonating-group method. A phenomenological imaginary potential, whose strength depends on whether the relative orbital angular momentum is even or odd, is included in the calculation in order to account approximately for open reaction channels. Exchange terms which arise from the nucleon-nucleon Coulomb interaction also are included. The introduction of both the odd-even absorption and the Coulomb-exchange terms is found to lead to significantly improved agreement with experiment. In addition, the use of improved rms matter radii for ^3He and ^3H is found to yield ^2P_J bound-state energies for the $^3He + ^4He$ and $^3H + ^4He$ systems which are more consistent with experiment than found previously.

[NUCLEAR STRUCTURE, REACTIONS ^7Li, ^7Be; calculated ^2P_J, ^2F_J levels. $^4He(^3He, ^3He)$, $E_{c.m.} = 1.7 - 44.5$ MeV; calculated $\sigma(\Theta)$; deduced imaginary-potential strength, space-exchange mixture. Resonating-group method.]

I. INTRODUCTION

Single-channel resonating-group calculations have achieved some success in reproducing $^3He + ^4He$ elastic scattering data over a wide range of energies,[1-8] and at 44.5 MeV (c.m.)[9] a fit to the elastic differential-cross-section data[8] was improved considerably by the inclusion in the theory[10] of a phenomenological local imaginary potential in order to account for effects of reaction channels on the elastic channel. Furthermore, resonating-group calculations with local absorptive potentials have been fairly successful in describing $^3He + ^3He$ elastic scattering[11] and $\alpha + \alpha$ elastic scattering[12] at energies above their respective reaction thresholds. More recently, a simple nonlocality has been introduced into the imaginary potential through the inclusion of a Majorana (space-exchange) component. This results in an odd-even orbital-angular-momentum dependence of the absorptive potential. In studies of the $p + \alpha$ system[13] and $^3He + ^3He$ system[14] this modification aided in obtaining good agreement between theory and the elastic scattering data over a wide range of energies. In addition, a Majorana component in the imaginary potential has been employed[15] in an optical-model fit to differential-cross-section and polarization data for the scattering of 30-MeV protons from ^{40}Ca. In that analysis[15] it was found that the presence of the Majorana component considerably improved the backward-angle fits to both the differential-cross-section and polarization data. In the present work, therefore, we include such a component in our absorptive potential.

In previous[1,3,10] resonating-group calculations for the $^3He + ^4He$ and $^3H + ^4He$ systems, the Coulomb interaction between the two clusters was obtained with the use of an unantisymmetrized wave function. This results in the omission from the calculation of Coulomb-exchange terms, which would affect the nonlocal part of the effective nucleus-nucleus interaction obtained from the resonating-group method. Generally, the Coulomb-exchange terms have a nonnegligible influence on the calculated properties of the system. It has been pointed out,[16] however, that, for the $\alpha + \alpha$ system which contains only even relative orbital angular momenta between the clusters, the effect of the Coulomb-exchange terms can be simulated by an adjustment of the exchange mixture in the employed nucleon-nucleon potential. On the other hand, it has been found[17] that for a system such as $p + \alpha$, in which both even and odd relative orbital angular momenta can exist between the clusters, the Coulomb-exchange interaction in states of even angular momenta is significantly different from that in states of odd angular momenta. Moreover, this odd-even feature of the Coulomb-exchange interaction cannot be reproduced by an adjustment of the nucleon-nucleon exchange mixture. Because of the possibility that such an odd-even effect would also be present in the $^3He + ^4He$ and $^3H + ^4He$ systems, we have included the Coulomb-exchange terms in the present calculation. Indeed, we find that these terms also produce such an odd-even effect here and that their inclusion results in improved agreement

with experiment.

Other improvements we make here over previous calculations for the ^{3}He + ^{4}He and ^{3}H + ^{4}He systems[1,3,10] are the use of a nucleon-nucleon potential (potential B of Ref. 18; see also Refs. 11–14) which fits better the low-energy nucleon-nucleon data and the use of more consistently determined matter size parameters for the ^{3}He and ^{3}H nuclei (see Appendix A).

With the inclusion of the above-mentioned improvements in the present resonating-group calculation, we have obtained rather good fits to the spin-orbit-averaged energies of the ^2P_J bound states of ^{7}Li and ^{7}Be and to ^{3}He + ^{4}He elastic scattering differential-cross-section data[4–6,7,8,19] at 16 energies from 1.7 to 44.5 MeV. The elastic scattering fits were obtained with only two energy-dependent parameters, the depth of the imaginary potential, and the strength of its space-exchange component. The energy range from 2 to 10 MeV was not included in the present analysis because phase-shift splittings due to noncentral forces are very important in this energy region,[3,20] and our calculation is performed with a central nucleon-nucleon potential.

Section II contains a brief formulation of the calculation, and in Sec. III the present results are compared with experiment. In Sec. IV a discussion is presented of a proposed effective interaction between the ^{4}He and ^{3}He nuclei. There the odd-even features of the interaction are stressed. Section V contains a summary and conclusions, and the Appendixes contain the results of the Coulomb-exchange calculation and describe the determination of the rms matter radii for ^{4}He, ^{3}He, and ^{3}H.

II. FORMULATION

The basic formulation of the one-channel resonating-group description of the ^{3}He + ^{4}He and ^{3}H + ^{4}He systems has been given previously,[1,3,10] and therefore only a brief discussion of the formalism is presented here. The most important features of the resonating-group method are: (i) a variational principle is used to calculate the relative motion function $F(\vec{r})$ for the two interacting nuclei; (ii) the seven-particle trial wave function for the system is completely antisymmetrized and is of the form $\mathcal{A}[\Phi_4\Phi_3 F(\vec{r})]$, where $\mathcal{A}$ is an antisymmetrization operator and Φ_4 and Φ_3 describe the internal states of the two interacting nuclei; and (iii) in the employed seven-particle Hamiltonian operator a nucleon-nucleon potential is used which reproduces the nucleon-nucleon effective-range parameters.

The internal functions Φ are *not* varied in the calculation, only the relative function $F(\vec{r})$ is varied. The spatial parts φ_4 and φ_3 of the internal functions are taken to be of the Gaussian forms

$$\varphi_4 = \exp[-\tfrac{1}{2}\alpha \sum_{i=1}^{4} (\vec{r}_i - \vec{R}_4)^2],$$

$$\varphi_3 = \exp[-\tfrac{1}{2}\bar{\alpha} \sum_{i=5}^{7} (\vec{r}_i - \vec{R}_3)^2] . \quad (1)$$

The width parameters α, $\bar{\alpha}(^3\mathrm{He})$, and $\bar{\alpha}(^3\mathrm{H})$ of Eq. (1) are chosen to give the correct rms matter radii for the respective nuclei. These parameters and the associated rms radii are given in Table I, and the extraction of the matter radii from the measured charge form factors is described in Appendix A.

The nucleon-nucleon potential we use here is not that of Refs. 1, 3, 10, but is instead the improved potential B of Ref. 18, which has been used in recent resonating-group calculations for other systems.[11–14,17,21] The two depth parameters and two range parameters of this central potential are chosen to reproduce the nucleon-nucleon effective-range parameters. The other parameter in the potential is a dimensionless quantity u, which determines the space-exchange mixture in the potential, but which does not affect the effective-range parameters. The value $u = 1$ corresponds to a pure Serber exchange mixture. As mentioned previously,[17,21] the quantity u is treated as an adjustable parameter in order partially to compensate for defects in the calculation, principally the lack of inclusion of specific distortion effects.[22] Because the two-nucleon scattering data favor a near-Serber exchange mixture for the nucleon-nucleon potential, the value of u finally adopted should be reasonably close to 1. The criterion used here to determine u is to choose the value which best fits the energies of the ^2P_J bound states of ^{7}Li and ^{7}Be (see Sec. III).

With the introduction of a phenomenological imaginary potential iW into the resonating-group formalism, the relative-motion function $F(\vec{r})$ satisfies an integrodifferential equation of the form

$$\left[\frac{\hbar^2}{2\mu}\nabla^2 + E - V_D(r) - V_C(r) - iW\right] F(\vec{r}) = \int K(\vec{r},\vec{r}\,')F(\vec{r}\,')\,d\vec{r}\,', \quad (2)$$

where μ is the reduced mass and E is the c.m. kinetic energy at large cluster separation. The direct nuclear potential $V_D(r)$, the direct Coulomb potential $V_C(r)$, and the kernel function $K(\vec{r},\vec{r}\,')$ are given by the resonating-group method and

depend not only on the form chosen for the internal functions Φ, but also on the nucleon-nucleon potential used. Because the nucleon-nucleon potential we employ here is not the same as that of Refs. 1, 3, 10, the forms of $V_D(r)$, $V_C(r)$, and $K(\vec{r},\vec{r}\,')$ in Eq. (2) are not the same as given in Ref. 1. However, the required modifications to the formulas of Ref. 1 are not complicated and can be carried out in the manner indicated in the Appendix of Ref. 17. In addition to the kernel terms used in Refs. 1, 3, 10, we here include those terms in $K(\vec{r},\vec{r}\,')$ which arise from the nucleon-nucleon Coulomb interaction. These Coulomb-exchange contributions to the kernel are given in Appendix B.

The imaginary potential in Eq. (2) is taken to be of the form

$$W=(1+C_I P^r)U(r)\,, \tag{3}$$

where P^r is a Majorana operator which exchanges the position of the c.m. of the α particle with that of the mass-3 particle, C_I is an adjustable parameter, and $U(r)$ is given by

$$U(r)=-U_0\left[\frac{1}{1+e^{(r-R)/a}}+\frac{4e^{(r-R)/a}}{(1+e^{(r-R)/a})^2}\right], \tag{4}$$

with

$$R=3.2\text{ fm},\quad a=0.5\text{ fm}. \tag{5}$$

Equation (3) has been used successfully in studies of the $p+\alpha$ system[13] and the ^{3}He + ^{3}He system[14] over a broad range of energies. The use of the exchange term $C_I P^r$ in Eq. (3) is a simple way of including some nonlocality in the imaginary potential, which in principle should be nonlocal.[23] Further rationale for the introduction of this exchange term, which causes an odd-even orbital-angular-momentum dependence of the imaginary potential, is given in Refs. 13 and 24. The spatial form of the imaginary potential, as given by Eq. (4), is of a Woods-Saxon shape having equal volume and surface components, and, along with Eq. (5), was used previously[10] to study the ^{3}He + ^{4}He system. We have investigated the effects of changes from the values of Eq. (5) of the radius R and diffuseness a, and changes from the equal volume and surface component form of Eq. (4). No significant improvements in fits to elastic scattering data result from such changes.

With the nucleon-nucleon exchange parameter u fixed by the bound-state data and with the radius and diffuseness of the imaginary potential fixed by Eq. (5), there are only two energy-dependent parameters in the calculation. These are the strength of the imaginary potential, U_0 of Eq. (4), and the exchange constant in the imaginary potential, C_I of Eq. (3).

TABLE I. rms matter radii and width parameters α and $\bar{\alpha}$ [see Eq. (1)] for ^{4}He, ^{3}He, and ^{3}H (see Appendix A).

Nucleus	rms matter radius (fm)	Width parameter (fm^{-2})
^{4}He	1.481	0.514
^{3}He	1.650	0.367
^{3}H	1.627	0.378

III. RESULTS

A. Bound states

As was mentioned in Sec. II, the value of the exchange parameter u in the nucleon-nucleon potential is determined by reproducing as accurately as possible the energies of the ^2P_J bound states of the nuclei ^{7}Li and ^{7}Be. Each of these two nuclei has a $^2P_{3/2}$ ground state and a $^2P_{1/2}$ first excited state, both of which are bound with respect to breakup into ^{4}He plus the appropriate mass-3 particle. Because we use a purely central nucleon-nucleon potential, our calculation yields the same energy for the $J=\frac{3}{2}$ state as it does for the $J=\frac{1}{2}$ state. Therefore, for each nucleus we average the experimental energies of the ground state and first excited state, weighted according to the value of $\vec{l}\cdot\vec{s}$ for each state. This results in an averaged bound-state energy for ^{7}Li of 2.307 MeV below the ^{4}He + ^{3}H breakup threshold and for ^{7}Be of 1.443 MeV below the ^{4}He + ^{3}He breakup threshold, and it is these energies which are compared with the calculation. We find that, with a single value of u given by

$$u=0.984\,, \tag{6}$$

these two averaged energies are reproduced to within 13 keV. This agreement is significantly better than the 60-keV agreement found in a previous calculation[3] which did not include the Coulomb-exchange terms, which used a common value for the rms matter radius of ^{3}He and ^{3}H, and which used the previous, somewhat poorer, nucleon-nucleon potential. The largest part of this improvement is a consequence of the inclusion of the Coulomb-exchange terms.

The adjustment of the exchange-mixture parameter u is a phenomenological way to compensate for the omission of the specific distortion effect. It is certainly a rather crude procedure and will yield accurate results only in those cases where the specific distortion effect does not play

a dominant role. Thus, it is indeed gratifying that the resultant value for u turns out to be 0.984, which is rather close to the value of 0.92 required in the case of $\alpha+\alpha$ scattering for which the specific distortion effect has been shown to be unimportant.[25] The fact that a common value of u is capable of yielding consistent bound-state results in both ^{7}Li and ^{7}Be is not at all surprising, but rather should be expected. It is merely a reflection of the fact that specific distortion effects are very similar in these two mirror systems.

B. ^{3}He+^{4}He elastic scattering

In the present work we compare our calculated differential cross sections with experimental data[4-6,7,8,19] at 16 cm energies from 1.7 to 44.5 MeV. At a c.m. energy of 1.7 MeV, no reaction channels are open, and therefore, with the u of Eq. (6) having been determined from the bound-state data, no adjustable parameters are present in the calculation. The excellent agreement between theory and experiment[19] obtained at this energy is shown in Fig. 1.

In the c.m. energy region from about 2 to 10 MeV, phase-shift splittings due to noncentral forces are quite important[3,20]; in particular, strong $^2F_{7/2}$ and $^2F_{5/2}$ resonances occur. Hence, detailed comparisons of our calculated differential cross sections with experiment cannot be made in this energy region, but could only be made if noncentral forces were to be included in the calculation. We can, however, compare our calculated ^{7}Li and ^{7}Be ^2F_J resonance energies with the $\vec{l}\cdot\vec{s}$ weighted average of the experimental $^2F_{7/2}$ and $^2F_{5/2}$ resonance energies. We find that the present calculated resonance energies are about 0.4 MeV higher than the averaged experimental energies. This is to be compared with the previous calculation[3] which gave about 0.6 MeV for this energy difference.

It appears from the calculation of Ref. 8 that, at energies above the ^2F_J resonance region, noncentral forces play only a minor role in the elastic scattering. We therefore expect that our use of a purely central nucleon-nucleon potential will not cause major difficulties above 10 MeV. The

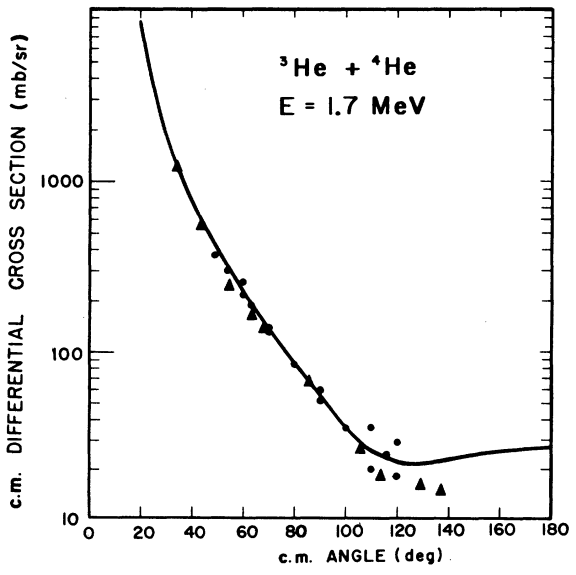

FIG. 1. Comparison with experimental data of the present calculation (solid curve) for ^{3}He + ^{4}He elastic scattering at a c.m. energy of 1.7 MeV. The circles represent the data of Miller and Phillips (Ref. 19) and the triangles represent the data of Chuang (Ref. 19).

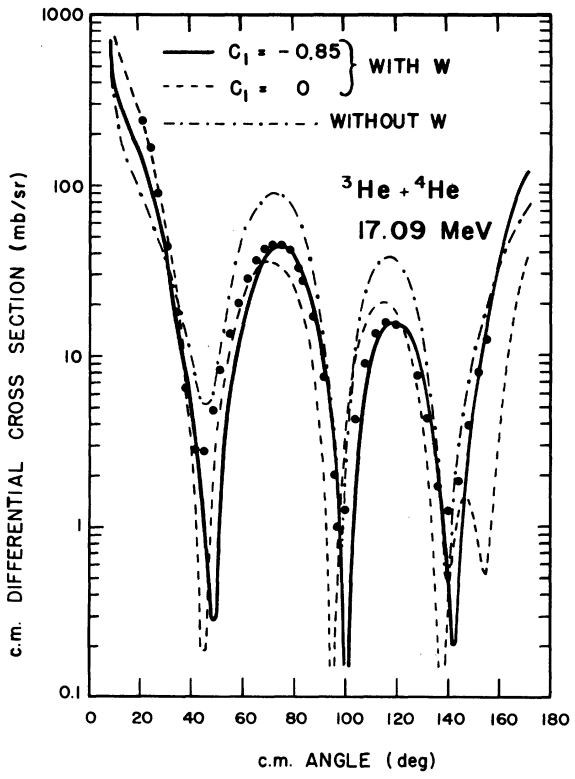

FIG. 2. Comparison of the present calculation (curves) with experimental (Ref. 5) data (points) for ^{3}He + ^{4}He elastic scattering at a c.m. energy of 17.09 MeV. The dot-dashed curve represents a calculation with no imaginary potential, the dashed curve represents a calculation with an imaginary potential with no Majorana component, and the solid curve represents a calculation with the full imaginary potential of Eqs. (3) – (5) employing the parameters of Table II.

procedure we employ at these higher energies is to calculate the differential cross section at each energy for a range of values of U_0 [Eq. (4)] and C_I [Eq. (3)] and to choose those values which produce the best visual fit to the experimental data. Figure 2 compares three calculated curves with experimental data[5] at 17.09 MeV. The purpose of this figure is to show the general effects on the calculated differential cross section produced by the inclusion of an imaginary potential both with and without a space-exchange component. The dot-dashed curve in Fig. 2 represents the calculation with no imaginary potential, and this calculation is seen to yield too large a cross section at most angles, thereby indicating the need for absorption in the theory. The dashed curve illustrates the best fit obtainable when an imaginary potential with no space-exchange component is used. Here the two main areas of disagreement with experiment are the poor fit at backward angles and the failure to fit the cross sections at the two maxima near 75 and 115°. The solid curve shows the marked improvement in fit which occurs in both these areas when a space-exchange component is included in the imaginary potential.

In Table II we list the values of U_0 and C_I which, at each of the 16 energies considered, give the best visual fit to the experimental data. Also listed at each energy is the calculated total reaction cross section σ_R. The uncertainties given for U_0 and C_I correspond to the ranges over which these parameters can be varied before the quality of the fit is significantly worsened. The resulting uncertainties in σ_R are also given. In Figs. 3–5 are shown comparisons with experimental data (points) of the best fits (solid curves) obtained at 9 representative energies. The dashed curves at 10.14 MeV (Fig. 3) and 24.36 MeV (Fig. 4) indicate the best fits at these two energies when the

TABLE II. Values of C_I [Eq. (3)], U_0 [Eq. (4)], and total reaction cross section σ_R obtained at each c.m. energy E analyzed in the present work.

E (MeV)	C_I	U_0 (MeV)	σ_R (mb)
1.70	0	0	0
10.14	−0.50 ± 0.30	0.95 ± 0.10	294 ± 25
11.39	−0.50 ± 0.30	1.10 ± 0.20	306 ± 40
12.53	−0.65 ± 0.30	1.15 ± 0.25	296 ± 50
13.66	−0.70 ± 0.20	1.00 ± 0.10	261 ± 20
14.81	−0.75 ± 0.20	1.10 ± 0.15	274 ± 30
15.95	−0.75 ± 0.20	1.15 ± 0.20	285 ± 40
17.09	−0.85 ± 0.15	1.45 ± 0.20	318 ± 70
18.51	−0.75 ± 0.25	1.70 ± 0.25	372 ± 50
20.95	−0.55 ± 0.35	2.10 ± 0.25	449 ± 45
22.77	−0.60 ± 0.25	2.35 ± 0.20	461 ± 40
24.36	−0.60 ± 0.15	2.50 ± 0.20	465 ± 25
32.00	−0.45 ± 0.10	2.80 ± 0.20	448 ± 20
37.00	−0.45 ± 0.10	3.15 ± 0.10	444 ± 10
41.00	−0.45 ± 0.10	3.45 ± 0.15	445 ± 20
44.50	−0.55 ± 0.10	3.95 ± 0.25	447 ± 20

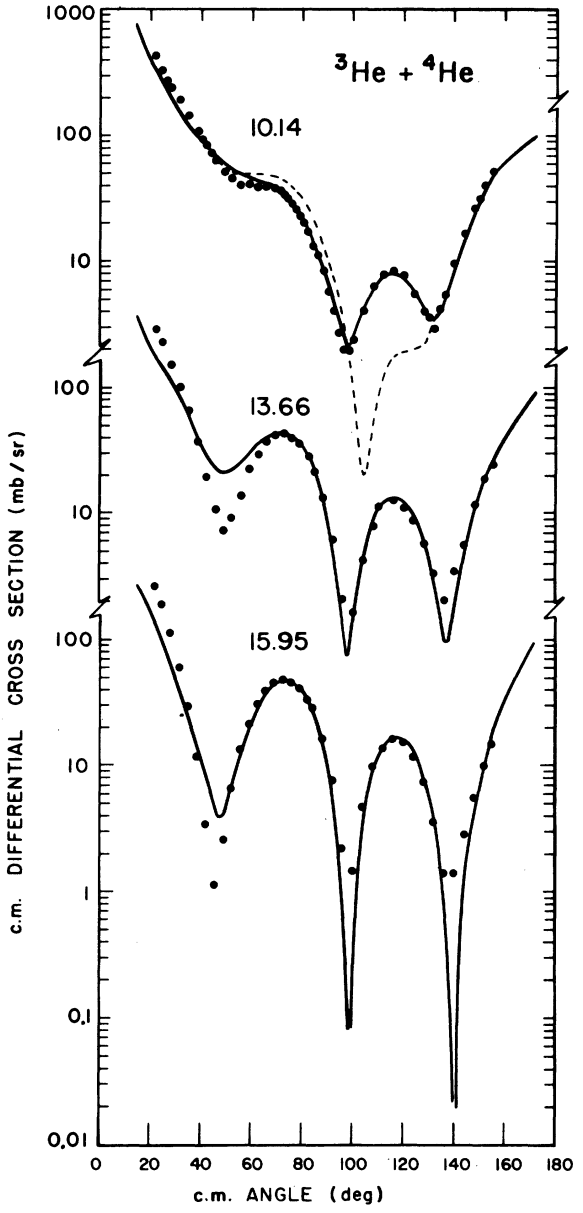

FIG. 3. Comparison of the present calculation (curves) with the data of Jacobs and Brown (Ref. 5) for ^{3}He + ^{4}He elastic scattering at c.m. energies of 10.14, 13.66, and 15.95 MeV. The imaginary potential of Eqs. (3) – (5) was used along with the parameters of Table II. The dashed curve illustrates the best fit obtainable at 10.14 MeV when no Coulomb-exchange terms are included in the calculation.

Coulomb-exchange terms are omitted from the calculation. Clearly there is a significant improvement in fit when the Coulomb-exchange terms are included. At other energies such improvements also occur although they are not always so striking as at the two energies shown. A general comparison in Figs. 3–5 of the solid curves with the data points illustrates that the present calculation, with only two energy-dependent parameters, does reproduce the experimental data fairly well over a broad energy range. In Figs. 3 and 4 the angular region near 40° shows the largest discrepancy between theory and experiment. Although the general manner in which the differential cross section in this angular region changes shape with increasing energy is well reproduced

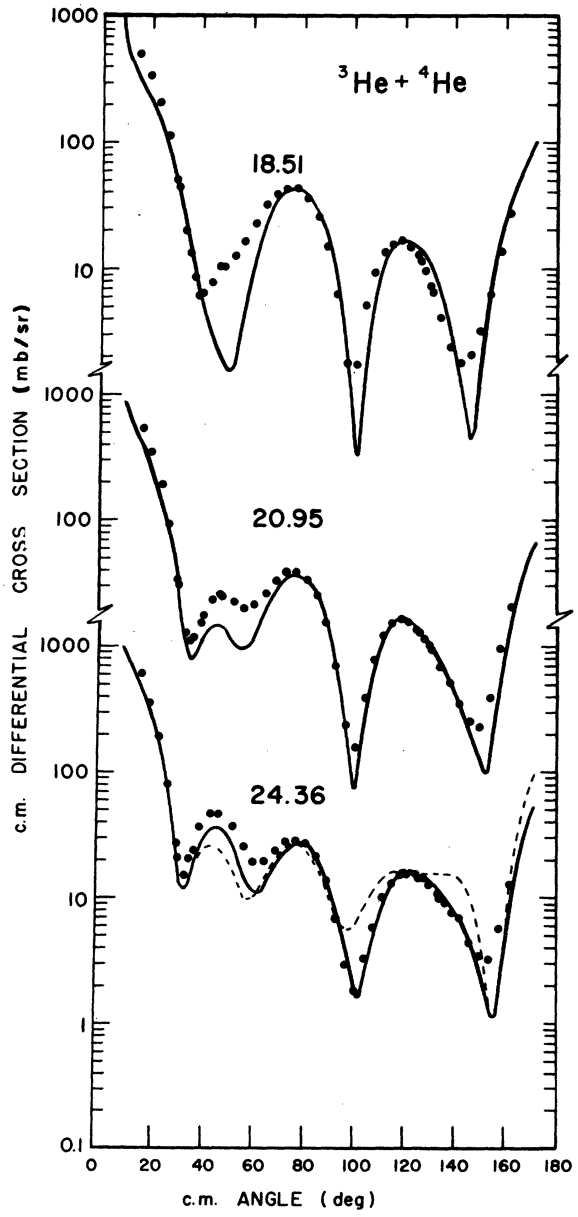

FIG. 4. Comparison of the present calculation (curves) with the data of Schwandt *et al.* (Ref. 4) for ^{3}He + ^{4}He elastic scattering at c.m. energies of 18.51, 20.95, and 24.36 MeV. The imaginary potential of Eqs. (3) – (5) was used along with the parameters of Table II. The dashed curve illustrates the best fit obtainable at 24.36 MeV when no Coulomb-exchange terms are included in the calculation.

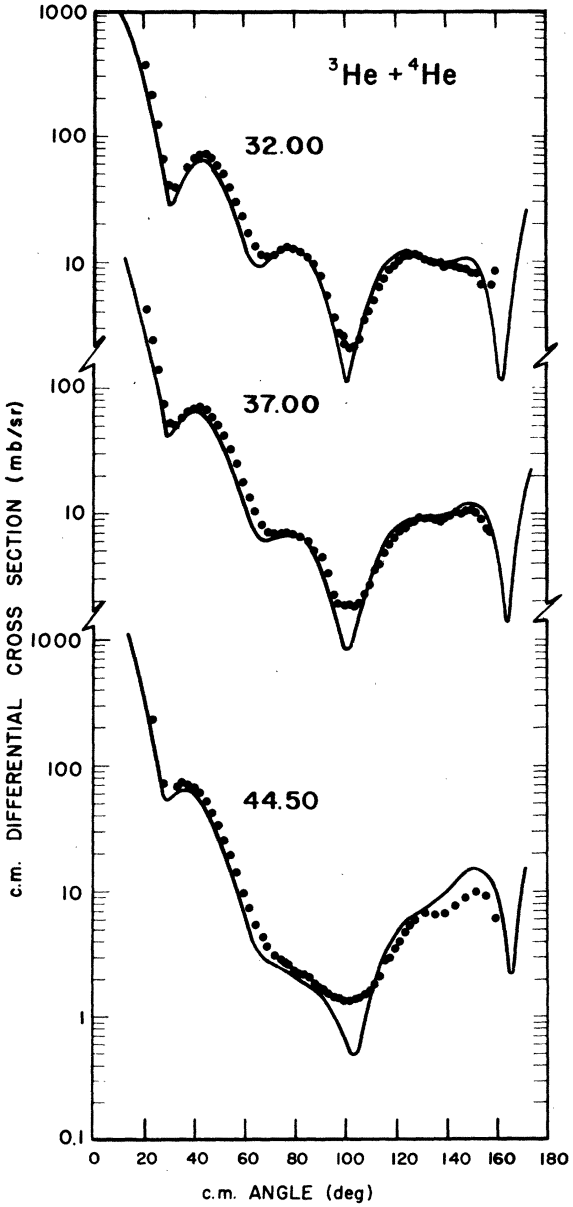

FIG. 5. Comparison of the present calculation (curves) with the data of Fetscher *et al.* (Ref. 8) for ^{3}He + ^{4}He elastic scattering at c.m. energies 32.00, 37.00, and 44.50 MeV. The imaginary potential of Eqs. (3) – (5) was used along with the parameters of Table II.

by the calculation, we note that the energies at which the calculated and experimental curves begin to show a maximum near 40° differ somewhat. Such problems with energy dependences of differential cross sections have been observed in other resonating-group calculations.[26] An additional area of noticeable discrepancy is present in Fig. 5 in the angular region near 100°, where the calculated relative minimum in the cross section has a much lower value than does the experimental minimum. Two effects not included in the present calculation are known to produce shallower cross-section minima. These are the use of noncentral forces, as was done in a study of the $p+\alpha$ system,[17] or the use of a two-Gaussian wave function to improve the description of the ^{3}He nucleus, as was done in a study of the $p+^3$He system.[21] In addition, the angular region in question is the region where interference between the direct amplitude and exchange amplitudes is important,[27] and therefore even small defects in the calculation could show up rather strongly in this region. An assessment of the relative importance of these possibilities will require further investigation.

A final comparison with experiment is shown in Fig. 6. The data[6] at 173.2° were measured in order to test the resonating-group prediction[5,28]

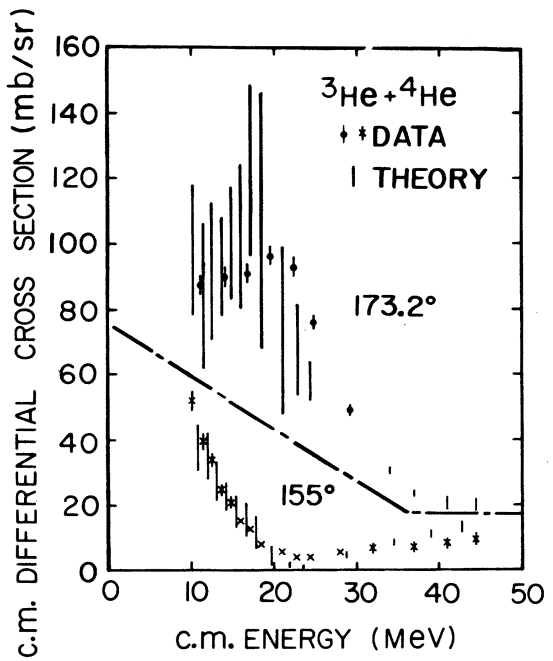

FIG. 6. Comparison of the present calculation (vertical bars) with experimental data at c.m. angles of 173.2° (Ref. 6) and 155° (Refs. 4, 5, 8). Some of the 155° points were interpolated from data at nearby angles. The length of the bars reflects the uncertainty in the calculation produced by the uncertainties in the imaginary-potential parameters of Table II.

of a sharply backward-peaked resonance structure in the differential cross section. The prediction of this structure arises from the exchange terms present in the calculation due to the use of a completely antisymmetrized wave function. In Ref. 6 the data were compared with a calculation which employed the previous nucleon-nucleon potential (see Sec. II) and which did not include Coulomb-exchange terms or an imaginary potential. In that comparison the calculated cross section showed a more marked structure than the experimental cross section and rose to a peak cross-section value of about twice that of experiment. The cross sections of the present calculation, which are shown in Fig. 6, give a better fit to the 173.2° data than did the calculation of Ref. 6. We should stress that the 173.2° data were not employed in the determination of the parameters of Table II, and therefore the calculation of the 173.2° excitation function can be regarded as a prediction made after the parameters of Table II are determined from angular distributions at fixed energies. The fact that the calculation in Fig. 6 is represented by bars rather than points is a reflection of the uncertainties in U_0 and C_I given in Table II. In Fig. 6 the 155° data and calculation are shown to illustrate the absence of the resonance structure at somewhat more forward angles.

In Tables III and IV we list the real parts and the imaginary parts, respectively, of the phase shifts we have calculated in the present work. Although our calculation does not yield perfect agreement with experiment, we feel that these phases should be useful as starting values in a phase-shift search on the elastic scattering data and would help to avoid the ambiguities inherent in phase-shift searches. In Table III we adopt the following convention[29] for the real parts of the phases:

$$\lim_{E\to 0}\delta_l=(n_b+n_f)\pi\ , \tag{7}$$

where n_b is the number of true bound states and n_f is the number of Pauli-forbidden bound states for states with orbital angular momentum l. For the ^{3}He + ^{4}He system we have $n_b=0$, $n_f=2$ for $l=0$; $n_b=1$, $n_f=1$ for $l=1$; $n_b=0$, $n_f=1$ for $l=2$; and $n_b=0$, $n_f=0$ for $l\geq 3$.

We conclude this section with some brief comments on other studies of the ^{3}He + ^{4}He system in the energy region considered here. Dunnill *et al.*[30] have performed an optical-model analysis of their ^{3}He + ^{4}He elastic scattering data at c.m. energies from about 7 to 11 MeV. It is difficult to make meaningful comments about their potential parameters, because they were not able to

TABLE III. Real parts of calculated phase shifts (deg) for ^{3}He + ^{4}He elastic scattering at c.m. energies E (MeV).

E	$l=0$	1	2	3	4	5	6	7	8	9	10	11
1.70	342.8	344.4	179.5	0.4	0	0	0	0	0	0	0	0
10.14	275.6	271.7	179.9	161.2	0.3	3.9	−0.3	0.2	0	0	0	0
11.39	268.4	265.3	179.3	161.3	1.4	5.9	−0.4	0.3	0	0	0	0
12.53	263.8	260.0	179.9	161.3	2.9	8.0	−0.4	0.5	−0.1	0	0	0
13.66	259.7	255.0	179.9	160.8	4.8	10.4	−0.5	0.7	−0.1	0	0	0
14.81	254.9	250.3	179.4	160.5	7.2	13.2	−0.5	1.0	−0.1	0.1	0	0
15.95	249.9	245.8	178.1	160.1	10.0	16.3	−0.4	1.3	−0.2	0.1	0	0
17.09	246.7	241.7	177.9	159.6	13.3	19.1	−0.2	1.7	−0.2	0.1	0	0
18.51	237.7	236.8	173.2	158.8	17.7	22.9	0.0	2.2	−0.2	0.2	0	0
20.95	227.1	229.0	167.9	157.3	25.0	30.1	0.8	3.4	−0.3	0.4	−0.1	0
22.77	221.2	223.7	165.4	156.0	32.0	34.8	1.6	4.4	−0.3	0.6	−0.1	0.1
24.36	216.4	219.3	163.2	154.9	38.1	39.6	2.4	5.3	−0.3	0.7	−0.1	0.1
32.00	197.4	201.4	153.9	149.5	64.0	64.7	8.3	11.0	0.5	2.0	−0.2	0.3
37.00	187.3	191.6	148.3	145.7	73.8	74.5	13.1	15.0	1.5	3.1	−0.1	0.6
41.00	180.2	184.7	144.2	142.7	78.4	79.2	17.3	18.2	2.6	4.1	0.1	0.9
44.50	174.3	179.3	140.6	140.3	80.6	82.6	21.3	20.1	3.8	5.1	0.3	1.2

obtain very good fits to the data. For example, the fit we obtain here at 10.14 MeV (Fig. 3) is considerably better than they obtained at a comparable energy. Vincent and Boschitz[31] have carried out an optical-model analysis of their 18-MeV (c.m.) data in which they attempted to fit the total reaction cross section σ_R as well as the elastic scattering differential cross section. Unfortunately they were led to assess the very large lower limit of 1300 mb to σ_R through an incorrect extrapolation to zero angle of the ^{3}He-breakup differential cross section (see footnote 16 of Ref. 10). In order to obtain such a large value of σ_R in their optical-model analysis, they were forced to employ an imaginary potential having what we consider an unrealistically large radial extent. Their resulting fit to the scattering data is reasonably good, however. Our interpretation of the data of Vincent and Boschitz[31] is that it yields a lower limit to the total reaction cross section of about 300 mb, which is consistent with Table II. Fetscher *et al.*[7,8] have measured ^{3}He + ^{4}He elastic scattering differential cross sections at c.m. energies from 28 to 44 MeV and have compared their data with a resonating-group calculation which included a nucleon-nucleon spin-orbit potential. They point out that the effect of this noncentral potential is only minor at the energies

TABLE IV. Imaginary parts of calculated phase shifts (deg) for ^{3}He + ^{4}He elastic scattering at c.m. energies E (MeV).

E	$l=0$	1	2	3	4	5	6	7	8	9	10	11
10.14	8.9	7.9	7.4	9.5	0.6	0.4	0	0	0	0	0	0
11.39	9.9	8.9	9.0	10.4	1.1	0.8	0	0	0	0	0	0
12.53	8.5	10.1	7.8	11.6	1.1	1.4	0	0	0	0	0	0
13.66	7.5	8.9	6.8	10.2	1.1	1.9	0	0	0	0	0	0
14.81	7.5	10.0	6.9	11.4	1.4	2.9	0	0.1	0	0	0	0
15.95	8.0	10.3	7.4	11.8	1.9	4.1	0.1	0.1	0	0	0	0
17.09	7.5	13.5	6.7	15.5	1.8	6.9	0.1	0.2	0	0	0	0
18.51	9.6	14.7	9.5	17.0	4.3	10.0	0.2	0.4	0	0	0	0
20.95	12.3	15.8	13.7	18.4	12.7	15.5	0.7	0.7	0	0	0	0
22.77	11.9	17.9	13.2	21.0	14.7	21.6	0.9	1.2	0.1	0.1	0	0
24.36	11.9	18.8	13.3	22.1	16.9	26.2	1.3	1.6	0.1	0.1	0	0
32.00	13.9	18.1	15.5	21.0	24.5	31.1	4.7	4.7	0.5	0.5	0.1	0
37.00	13.9	19.7	15.3	22.5	22.2	31.3	7.6	8.2	1.0	1.0	0.1	0.1
41.00	13.9	21.0	15.2	23.6	20.6	30.6	10.1	11.8	1.6	1.7	0.2	0.2
44.50	12.3	25.1	13.3	27.8	17.2	34.2	10.8	17.2	2.0	2.8	0.3	0.4

they consider. In addition, they have introduced phenomenological absorption factors into the calculation in an attempt to account for effects of reaction channels on the elastic channel. Their calculation shows qualitative agreement with experiment, but is a much less accurate reproduction of the data than we obtain here. This may be due to the fact that their absorption factors do not account for reactions nearly as well as does our imaginary potential; however their neglect of Coulomb-exchange terms and use of a nucleon-nucleon potential with a simpler central part than we use (see Sec. II) will also affect the quality of their fit.

IV. EFFECTIVE POTENTIAL

Because the resonating-group method is impractical to apply to all nuclear systems of interest, it is very useful to obtain on effective real potential V_{eff} which is simple enough to be readily used in elastic scattering analyses yet which contains the important features of the interaction given by the resonating-group calculation. To be precise, V_{eff} would be employed in an analysis by replacing Eq. (2) with the equation

$$\left[\frac{\hbar^2}{2\mu}\nabla^2 + E - V_{\text{eff}} - V_C(r) - iW\right]F(\vec{r}) = 0 \ . \tag{8}$$

In the expression adopted for V_{eff} it is particularly important that exchange effects be accounted for in some manner. It has been shown previously (see for example Fig. 2 of Ref. 10 and Fig. 2 of Ref. 24) that a striking manifestation of the exchange effects present in resonating-group calculations is an odd-even orbital-angular-momentum dependence of the real parts of the phase shifts, wherein the odd-l phases show a decreasing trend with increasing l which is distinctly different from that of the even-l phases. A similar odd-even dependence to the phase shifts can be given by a simple real potential containing a space-exchange component. In fact, it has been shown in a study of the $n+\alpha$ system[32] that an effective real potential V_{eff} of the form

$$V_{\text{eff}} = V_D(r) + V_a(r) + P^r V_b(r) \tag{9}$$

will, in the Born approximation, yield the same scattering amplitude as does the resonating-group calculation. In Eq. (9) $V_D(r)$ is as given in Eq. (2), P^r is a space-exchange operator as in Eq. (3), and $V_a(r)$ and $V_b(r)$ are energy-dependent potentials representing exchange processes. In an optical-model type analysis, Eq. (9) can be simplified somewhat by taking V_D, V_a, and V_b to have the same phenomenologically determined shape, and this would yield a V_{eff} of the form[24]

$$V_{\text{eff}} = (1 + C_R P^r) V_R(r) \ , \tag{10}$$

where C_R is an energy-dependent parameter.

In order to give a semiquantitative assessment of the importance of exchange processes for ^{3}He $+^4$He scattering in the energy region considered here, we have taken in Eq. (10)

$$V_R(r) = C_D V_D(r) \ , \tag{11}$$

where $V_D(r)$ is the direct nuclear potential of Eq. (2) and C_D is an energy-dependent constant. Deviations of C_D from unity and C_R from zero are measures of the strength of exchange processes. Values for C_D and C_R at each energy were obtained by choosing them to reproduce as well as possible the phase shifts given by the resonating-group calculation.[33] The degree to which this procedure reproduces the resonating-group phases is indicated in Fig. 2 of Ref. 10. The values obtained for C_D and C_R vary somewhat with energy, and these values averaged over the energy range 20 to 50 MeV are

$$C_D = 1.13, \quad C_R = -0.17 \ . \tag{12}$$

At energies above 50 MeV, C_D and C_R decrease slowly in absolute magnitude with increasing energy. The values in Eq. (12) indicate that it is important to include exchange effects in the real potential, and the negative value of C_R shows that the effective real potential is more attractive in odd-l states than in even-l states. It is of interest to note here that Votta *et al.*[34] have successfully used a Majorana component in the real optical potential to fit elastic scattering data of 85-MeV protons on ^{3}He and ^{4}He.

Because of the success we have had here and for other systems with an imaginary potential containing a space-exchange component, it is proposed that in general the imaginary part of the effective potential be given the form of Eq. (3), in which, lacking a microscopic model, one would attempt to determine $U(r)$ on a phenomenological basis. On comparing the values of C_I in Table II with the value of C_R in Eq. (12) we observe that the sign of C_I is the same as that of C_R and that the magnitude of C_I is about 3 to 5 times that of C_R. The equality of the signs of C_I and C_R and a large value for the ratio C_I/C_R have also been found to occur in resonating-group studies of the light systems $p+\alpha$ (Ref. 13) and ^{3}He $+^3$He (Ref. 14) and in an optical-model analysis of the $p+^{40}$Ca system.[15] In contrast to the parameter C_R, we have no microscopic model for determining C_I, and therefore at present we offer no explanation for these empirically determined relationships between the two exchange parameters.

V. CONCLUSION

Into the present study of the ^{3}He + ^{4}He and ^{3}H + ^{4}He systems we have incorporated the following improvements over previous calculations[1,3]: use of improved rms matter radii for the mass-3 nuclei, use of an improved nucleon-nucleon potential, inclusion of Coulomb-exchange terms, and use of an imaginary potential containing a Majorana component. The present calculation reproduces rather well bound-state and scattering data over a wide energy range. Particularly satisfying is the success in calculating the experimentally observed rise in the elastic scattering differential cross section at backward angles, which implies[10] that exchange processes are accounted for in a reasonably correct manner.

As in other single-channel resonating-group calculations, we have found that the introduction of an odd-even orbital-angular-momentum dependence into the imaginary potential results in an improved fit to experiment. With the presence of this feature, satisfactory agreement between theory and experiment, in particular around the diffraction maxima and at backward angles, can now be obtained over a wide energy range.

The Coulomb-exchange terms are found to be particularly important for the bound-state calculation and at energies around 10 and 24 MeV. The reason is probably that the contribution from these terms becomes especially large in energy regions where resonance levels exist. Indeed, a simple R-matrix analysis of the calculated phase shifts does give an indication of the existence of a broad $l=2$ level near 10 MeV, and of both an $l=4$ and an $l=5$ resonance level near 24 MeV.

We have also indicated here that a simple real potential containing a Majorana component is a reasonable type of potential to employ in lieu of performing a full resonating-group calculation. In fact, this type of real potential has been used recently in optical-model analyses.[15,34] Finally, we wish to state the possibility, which has also been mentioned elsewhere,[15,24] that exchange processes in heavy-ion scattering may be rather well accounted for through the use of an effective interaction which contains Majorana components in both its real and imaginary parts.

We wish to thank Dr. Ch. Weddigen for sending us the numerical values of his experimental results.

APPENDIX A: rms MATTER RADII

In this Appendix we use information obtained from electron scattering data to determine the rms matter radii of the nuclei ^{4}He, ^{3}He, and ^{3}H. Two types of nuclear form factor $F(q^2)$ are involved in this determination: the charge form factor $C(q^2)$, which is the Fourier transform of the nuclear charge density, and the body form factor $B(q^2)$, which is the Fourier transform of the nuclear matter density. With the exception of the charge form factor of the neutron, these form factors are related to the appropriate ms radii $\langle r^2\rangle$ through the low-q^2 expansion[35]

$$F(q^2)=1-\tfrac{1}{6}\langle r^2\rangle q^2+\cdots \tag{A1}$$

and for the neutron the expansion is

$$C_n(q^2)=-\tfrac{1}{6}\langle r^2\rangle_n^c q^2+\cdots . \tag{A2}$$

The nucleon ms radii needed in the present analysis are obtained from a consideration of the low-q^2 expansion of the quantities $G_{ES}=\frac{1}{2}[C_p(q^2)+C_n(q^2)]$ and $G_{EV}=\frac{1}{2}[C_p(q^2)-C_n(q^2)]$ of Janssens *et al.*[36] The following charge form factors for low q^2 are obtained:

$$C_p(q^2)=1-0.120\,48\,q^2+\cdots , \tag{A3}$$

$$C_n(q^2)=+0.021\,16\,q^2+\cdots , \tag{A4}$$

where q is in units of fm^{-1}. Equations (A1) through (A4) yield, for the nucleon ms radii:

$$\langle r^2\rangle_p^c=0.7229\ \text{fm}^2, \quad \langle r^2\rangle_n^c=-0.1270\ \text{fm}^2 . \tag{A5}$$

First we determine the ^{4}He rms matter radius. The body form factor $B_\alpha(q^2)$ is related to the charge form factor $C_\alpha(q^2)$ by the following simple relation[37,38]:

$$B_\alpha(q^2)=\frac{C_\alpha(q^2)}{C_p(q^2)+C_n(q^2)} . \tag{A6}$$

Upon making a low-q^2 expansion of Eq. (A6) and employing Eqs. (A1) and (A2) we obtain the following equation for the ms matter radius $\langle r^2\rangle_\alpha$ of the ^{4}He nucleus:

$$\langle r^2\rangle_\alpha=\langle r^2\rangle_\alpha^c-\langle r^2\rangle_p^c-\langle r^2\rangle_n^c . \tag{A7}$$

We take the ms charge radius to be $\langle r^2\rangle_\alpha^c=(1.67\ \text{fm})^2$, which is consistent with the electron scattering data.[39,40] Equations (A5) and (A7) then yield the result

$$\langle r^2\rangle_\alpha^{1/2}=1.481\ \text{fm}, \tag{A8}$$

and use of Eq. (8) of Ref. 3 yields the width parameter $\alpha=0.514$ fm^{-2} listed in Table I.

Finally, we discuss the determination of the rms matter radii for the nuclei ^{3}He and ^{3}H. Schiff[41] gives the following equations relating the charge form factors and body form factors for ^{3}He(τ) and ^{3}H(t), respectively (we drop the argument q^2):

$$2C_\tau=2C_p(B_\tau-\tfrac{1}{3}B_\tau')+C_n(B_\tau+\tfrac{2}{3}B_\tau'), \tag{A9}$$

$$C_t=2C_n(B_t-\tfrac{1}{3}B_t')+C_p(B_t+\tfrac{2}{3}B_t'), \tag{A10}$$

where the body form factors B arise from the S-state part of the mass-3 wave function, and the body form factors B' arise from the product of the S-state part with the S'-state part of the mass-3 wave function. The form factors B' are considerably smaller in magnitude than the form factors B (see Fig. 4 of Ref. 41), and it is a good approximation to set $B_t' = B_\tau'$ (see footnote 6 of Ref. 41). The B' can then be eliminated from Eqs. (A9) and (A10) to yield

$$2C_\tau + C_t = C_p(2B_\tau + B_t) + C_n(B_\tau + 2B_t)\,. \tag{A11}$$

On applying Eqs. (A1) and (A2) to Eq. (A11) we obtain

$$\tfrac{2}{3}\langle r^2\rangle_\tau + \tfrac{1}{3}\langle r^2\rangle_t = r_0^{\,2}\,, \tag{A12}$$

with

$$r_0^{\,2} = \tfrac{2}{3}\langle r^2\rangle_\tau^c + \tfrac{1}{3}\langle r^2\rangle_t^c - \langle r^2\rangle_p^c - \langle r^2\rangle_n^c = 2.6987\ \text{fm}^2\,. \tag{A13}$$

The numerical value in Eq. (A13) is obtained through use of Eq. (A5) and by taking the values of the ms charge radii to be $\langle r^2\rangle_\tau^c = (1.87\ \text{fm})^2$ and $\langle r^2\rangle_t^c = (1.70\ \text{fm})^2$ as given by the data of Collard *et al.*[42] To determine individual values for the ms matter radii $\langle r^2\rangle_\tau$ and $\langle r^2\rangle_t$ a relationship between them in addition to the relationship of Eq. (A12) is needed. For this we use the following difference relation:

$$\langle r^2\rangle_\tau^{1/2} - \langle r^2\rangle_t^{1/2} = \delta = 0.0232\ \text{fm}. \tag{A14}$$

The numerical value in Eq. (A14) is obtained from a variational calculation for the mass-3 system and arises from the Coulomb repulsion between the two protons in ^{3}He. This type of calculation is described in Ref. 38, and the nucleon-nucleon potential we use for the determination of δ is the potential of Ref. 38 having a hard core of radius 0.45 fm. Although some error is expected in the magnitudes of the two rms radii calculated in this way, the difference δ should be determined rather well.[43] Equations (A13) and (A14) can be solved for the rms matter radii, giving

$$\langle r^2\rangle_\tau^{1/2} = (r_0^{\,2} - \tfrac{2}{9}\delta^2)^{1/2} + \tfrac{1}{3}\delta = 1.650\ \text{fm}\,,$$
$$\langle r^2\rangle_t^{1/2} = (r_0^{\,2} - \tfrac{2}{9}\delta^2)^{1/2} - \tfrac{2}{3}\delta = 1.627\ \text{fm}. \tag{A15}$$

On applying Eq. (8) of Ref. 3 to the values given in Eq. (A15), the width parameters of Table I are obtained.

APPENDIX B: COULOMB KERNEL

The Coulomb-exchange terms contribute a part $K^C(\vec{r},\vec{r}\,')$ to the kernel $K(\vec{r},\vec{r}\,')$ of Eq. (2). We list here the partial-wave expanded kernel $k_l^C(r,r')$ defined by

$$k_l^C(r,r') = 2\pi r r' \int_{-1}^{+1} K^C(\vec{r},\vec{r}\,')P_l(\mu)\,d\mu\,, \tag{B1}$$

where $P_l(\mu)$ is a Legendre polynomial, and μ is the cosine of the angle between $\vec{r}$ and $\vec{r}\,'$. In the following ϵ is the electronic charge, α and $\bar{\alpha}$ are as in Eq. (1), the error function Φ is defined by

$$\Phi(\nu) = \frac{2}{\sqrt{\pi}}\int_0^\nu e^{-t^2}\,dt, \tag{B2}$$

and the symbols a_i, b_i, c_i, e_i $(i = 1, 2, 3)$, and S_i are defined in Ref. 1. Before listing the kernels for the two systems ^{3}H + ^{4}He and ^{3}He + ^{4}He it is convenient to define the following quantities:

$$\beta_{mn} = m\alpha + n\bar{\alpha}\,, \tag{B3}$$

$$p_{12}^1 = \tfrac{2}{3}\left(\frac{\alpha\beta_{89}}{2\beta_{83}}\right)^{1/2}, \quad p_{15}^1 = \tfrac{1}{6}(2\beta_{11})^{1/2},$$

$$p_{16}^1 = \tfrac{2}{3}\left(\frac{\bar{\alpha}\beta_{89}}{2\beta_{29}}\right)^{1/2}, \quad p_{23}^1 = \frac{1}{6\pi}\left(\frac{2\alpha}{\pi}\right)^{1/2},$$

$$p_{26}^1 = 2\left(\frac{\alpha\bar{\alpha}\beta_{89}}{2\beta_{11}\beta_{23}}\right)^{1/2}, \quad p_{67}^1 = \frac{1}{6\pi}\left(\frac{2\bar{\alpha}}{\pi}\right)^{1/2}, \tag{B4}$$

$$p_{12}^2 = \frac{1}{6\pi}\left(\frac{\beta_{11}}{\pi}\right)^{1/2}, \quad p_{13}^2 = \tfrac{2}{3}\left(\frac{2\alpha\beta_{11}\beta_{23}}{10\alpha^2 + 15\alpha\bar{\alpha} + 3\bar{\alpha}^2}\right)^{1/2},$$

$$p_{15}^2 = (2\beta_{11})^{1/2}, \quad p_{17}^2 = \tfrac{2}{3}\left(\frac{2\beta_{11}\beta_{23}}{13\alpha + 15\bar{\alpha}}\right)^{1/2},$$

$$p_{34}^2 = p_{23}^1, \quad p_{37}^2 = \tfrac{2}{3}\left(\frac{2\alpha\beta_{23}}{3\beta_{11}}\right)^{1/2}, \tag{B5}$$

$$p_{12}^3 = \frac{1}{2\pi}\left(\frac{\beta_{11}}{\pi}\right)^{1/2}, \quad p_{14}^3 = \tfrac{1}{2}(3\beta_{11})^{1/2},$$

$$p_{15}^3 = (6\beta_{11})^{1/2}, \tag{B6}$$

and

$$q_i = |L_i\vec{r} + M_i\vec{r}\,'|\,, \quad i = 1 \text{ to } 14, \tag{B7}$$

with

$$L_1=\tfrac{6}{7}\beta_{48}\left(\frac{2\alpha}{\beta_{89}\beta_{83}}\right)^{1/2},\quad M_1=-L_1\frac{\beta_{41}}{\beta_{48}},$$

$$L_2=\tfrac{6}{7}(15\alpha+9\bar{\alpha})\left(\frac{\bar{\alpha}}{2\beta_{29}\beta_{89}}\right)^{1/2},\quad M_2=-L_2\frac{\beta_{19}}{15\alpha+9\bar{\alpha}},$$

$$L_3=6\left(\frac{\alpha\bar{\alpha}\beta_{11}}{2\beta_{23}\beta_{89}}\right)^{1/2},\quad M_3=L_3,$$

$$L_4=\tfrac{3}{7}(2\beta_{11})^{1/2},\quad M_4=-L_4,$$

$$L_5=\tfrac{6}{7}\beta_{15}\left[\frac{2\alpha\beta_{11}}{\beta_{23}(10\alpha^2+15\alpha\bar{\alpha}+3\bar{\alpha}^2)}\right]^{1/2},\quad M_5=L_5\frac{-\alpha+2\bar{\alpha}}{\beta_{15}},$$

$$L_6=\tfrac{3}{7}\beta_{93}\left[\frac{2\beta_{11}}{\beta_{23}(13\alpha+15\bar{\alpha})}\right]^{1/2},\quad M_6=L_6\frac{5\alpha-3\bar{\alpha}}{\beta_{93}},$$

$$L_7=\left(\frac{6\alpha\beta_{11}}{\beta_{23}}\right)^{1/2},\quad M_7=L_7,$$

$$L_8=\tfrac{1}{7}(6\beta_{11})^{1/2},\quad M_8=-L_8,$$

$$L_9=\tfrac{8}{7}(3\beta_{11})^{1/2},\quad M_9=\tfrac{6}{7}(3\beta_{11})^{1/2},$$

$$L_{10}=M_1,\quad M_{10}=L_1,\quad L_{11}=M_2,\quad M_{11}=L_2,$$

$$L_{12}=M_5,\quad M_{12}=L_5,\quad L_{13}=M_6,\quad M_{13}=L_6,$$

$$L_{14}=M_9,\quad M_{14}=L_9. \tag{B8}$$

With these definitions the Coulomb kernels $k_l^{Ct}(r,r')$ and $k_l^{C\tau}(r,r')$ for the $^3H+{}^4He$ and $^3He+{}^4He$ systems, respectively, are given by:

$$\begin{aligned}k_l^{Ct}(r,r')&=-2\pi\epsilon^2e_1e^{-(6/7)\alpha_1(r^2+r'^2)}\\&\times\left\{rr'\int_{-1}^{+1}\left[\tfrac{1}{2}p_{12}^1\left(\frac{\Phi(q_1)}{q_1}+\frac{\Phi(q_{10})}{q_{10}}\right)+\tfrac{2}{3}p_{26}^1\frac{\Phi(q_3)}{q_3}+\tfrac{1}{2}p_{15}^1\frac{1}{q_4}\right]e^{(6/7)c_1rr'\mu}P_l(\mu)\,d\mu+2p_{23}^1S_l(-\tfrac{6}{7}c_1)\right\}\\&-2\pi\epsilon^2e_2e^{-(6/7)\alpha_2(r^2+r'^2)}\left\{rr'\int_{-1}^{+1}\left[\tfrac{1}{3}p_{15}^2\frac{\Phi(q_4)}{q_4}+p_{13}^2\left(\frac{\Phi(q_5)}{q_5}+\frac{\Phi(q_{12})}{q_{12}}\right)+p_{37}^2\frac{\Phi(q_7)}{q_7}\right]\right.\\&\left.\times e^{(6/7)c_2rr'\mu}P_l(\mu)\,d\mu+p_{34}^2S_l(-\tfrac{6}{7}c_2)\right\}\\&-2\pi\epsilon^2e_3e^{-(6/7)\alpha_3(r^2+r'^2)}\left\{rr'\int_{-1}^{+1}\left[\tfrac{1}{4}p_{15}^3\frac{\Phi(q_8)}{q_8}+p_{14}^3\left(\frac{\Phi(q_9)}{q_9}+\frac{\Phi(q_{14})}{q_{14}}\right)\right]e^{(6/7)c_3rr'\mu}P_l(\mu)\,d\mu\right\}\end{aligned} \tag{B9}$$

and

$$\begin{aligned}k_l^{C\tau}(r,r')&=-2\pi\epsilon^2e_1e^{-(6/7)\alpha_1(r^2+r'^2)}\\&\times\left\{rr'\int_{-1}^{+1}\left[p_{12}^1\left(\frac{\Phi(q_1)}{q_1}+\frac{\Phi(q_{10})}{q_{10}}\right)+p_{16}^1\left(\frac{\Phi(q_2)}{q_2}+\frac{\Phi(q_{11})}{q_{11}}\right)+p_{26}^1\frac{\Phi(q_3)}{q_3}+p_{15}^1\frac{1}{q_4}\right]e^{(6/7)c_1rr'\mu}P_l(\mu)\,d\mu\right.\\&\left.+(p_{23}^1+p_{67}^1)S_l(-\tfrac{6}{7}c_1)\right\}-2\pi\epsilon^2e_2e^{-(6/7)\alpha_2(r^2+r'^2)}\\&\times\left\{rr'\int_{-1}^{+1}\left[p_{15}^2\frac{\Phi(q_4)}{q_4}+p_{13}^2\left(\frac{\Phi(q_5)}{q_5}+\frac{\Phi(q_{12})}{q_{12}}\right)+p_{17}^2\left(\frac{\Phi(q_6)}{q_6}+\frac{\Phi(q_{13})}{q_{13}}\right)+p_{37}^2\frac{\Phi(q_7)}{q_7}\right]e^{(6/7)c_2rr'\mu}\right.\\&\left.\times P_l(\mu)\,d\mu+2p_{12}^2S_l(-\tfrac{6}{7}c_2)\right\}-2\pi\epsilon^2e_3e^{-(6/7)\alpha_3(r^2+r'^2)}\\&\times\left[rr'\int_{-1}^{+1}p_{15}^3\frac{\Phi(q_8)}{q_8}e^{(6/7)c_3rr'\mu}P_l(\mu)\,d\mu+2p_{12}^3S_l(-\tfrac{6}{7}c_3)\right].\end{aligned} \tag{B10}$$

*Work supported in part by the U. S. Atomic Energy Commission.

[1]Y. C. Tang, E. Schmid, and K. Wildermuth, Phys. Rev. 131, 2631 (1963).

[2]E. J. Wurster-Kanellopoulos, Institute for Theoretical Physics, University of Tübingen, Technical Report No. BMwF-FB K67-69, 1967 (unpublished).

[3]R. E. Brown and Y. C. Tang, Phys. Rev. 176, 1235(1968).

[4]P. Schwandt, B. W. Ridley, S. Hayakawa, L. Put, and J. J. Kraushaar, Phys. Lett. 30B, 30 (1969).

[5]C. G. Jacobs, Jr., and R. E. Brown, Phys. Rev. C 1, 1615 (1970).

[6]R. E. Brown, E. E. Gross, and A. Van der Woude, Phys. Rev. Lett. 25, 1346 (1970).

[7]W. Fetscher, K. Sattler, N. C. Schmeing, E. Seibt, Ch. Weddigen, and E. J. Kanellopoulos, Phys. Lett. 34B, 171 (1971).

[8]W. Fetscher, E. Seibt, Ch. Weddigen, and E. J. Kanellopoulos, Phys. Lett. 35B, 31 (1971).

[9]All energies will be in the c.m. system unless otherwise specified.

[10]Y. C. Tang and R. E. Brown, Phys. Rev. C 4, 1979 (1971).

[11]R. E. Brown, I. Reichstein, and Y. C. Tang, Nucl. Phys. A178, 145 (1971).

[12]R. E. Brown and Y. C. Tang, Nucl. Phys. A170, 225 (1971).

[13]D. R. Thompson, Y. C. Tang, and R. E. Brown, Phys. Rev. C 5, 1939 (1972).

[14]D. R. Thompson, Y. C. Tang, J. A. Koepke, and R. E. Brown, Nucl. Phys. A201, 301 (1973).

[15]G. W. Greenlees, W. Makofske, Y. C. Tang, and D. R. Thompson, Phys. Rev. C 6, 2057 (1972).

[16]S. Okai and S. C. Park, Phys. Rev. 145, 787 (1966).

[17]I. Reichstein and Y. C. Tang, Nucl. Phys. A158, 529 (1970).

[18]I. Reichstein and Y. C. Tang, Nucl. Phys. A139, 144 (1969).

[19]P. D. Miller and G. C. Phillips, Phys. Rev. 112, 2048 (1958); L. S. Chuang, Nucl. Phys. A174, 399 (1971).

[20]R. J. Spiger and T. A. Tombrello, Phys. Rev. 163, 964 (1967).

[21]I. Reichstein, D. R. Thompson, and Y. C. Tang, Phys. Rev. C 3, 2139 (1971).

[22]Specific distortion effects have been taken into account in the $d+\alpha$ system by H. Jacobs, K. Wildermuth, and E. Wurster, Phys. Lett. 29B, 445 (1969), and by D. R. Thompson and Y. C. Tang, Phys. Rev. C 8, 1649 (1973). In the latter reference a thorough discussion of the role of the exchange parameter u is given.

[23]H. C. Benöhr and K. Wildermuth, Nucl. Phys. A128, 1 (1969).

[24]R. E. Brown, Y. C. Tang, and D. R. Thompson, in *Few Particle Problems in the Nuclear Interaction,* edited by I. Šlaus, S. A. Moszkowski, R. P. Haddock, and W. T. H. van Oers (North-Holland, Amsterdam, 1972), p. 703.

[25]L. C. Niem, P. Heiss, and H. H. Hackenbroich, Z. Phys. 244, 346 (1971).

[26]See, for example, reference to an $l=3$ resonance in the ^{3}He+^{3}He system in J. G. Jenkin, W. D. Harrison, and R. E. Brown, Phys. Rev. C 1, 1622 (1970).

[27]See, for example, a discussion of the $n+\alpha$ system in D. R. Thompson and Y. C. Tang, Phys. Rev. C 4, 306 (1971).

[28]Y. C. Tang, in *Proceedings of the International Conference on Clustering Phenomena in Nuclei, Bochum, Germany, 1969* (International Atomic Energy Agency, Vienna, Austria, 1969), p. 109.

[29]V. G. Neudachin, V. I. Kukulin, V. L. Korotkikh, and V. P. Korennoy, Phys. Lett. 34B, 581 (1971); P. Swan, Proc. Roy. Soc. (Lond.) 228, 10 (1955); Ann. Phys. (N. Y.) 48, 455 (1968).

[30]F. Dunnill, T. J. Gray, H. T. Fortune, and N. R. Fletcher, Nucl. Phys. A93, 201 (1967).

[31]J. S. Vincent and E. T. Boschitz, Nucl. Phys. A143, 121 (1970).

[32]See Ref. 27.

[33]For convenience, no imaginary potential was included in making these comparisons. This procedure is valid because the absorptive strengths used here do not markedly affect the values of the real parts of the phase shifts (see Table I of Ref. 10).

[34]L. G. Votta, R. A. Stafford, P. G. Roos, N. S. Chant, and R. Woody, Bull Am. Phys. Soc. 18, 19 (1973).

[35]R. Hofstadter, Rev. Mod. Phys. 28, 214 (1956).

[36]T. Janssens, R. Hofstadter, E. B. Hughes, and M. R. Yearian, Phys. Rev. 142, 922 (1966).

[37]S. C. Jain and B. K. Srivastava, Phys. Rev. 164, 1226 (1967).

[38]Y. C. Tang and R. C. Herndon, Phys. Lett. 18, 42 (1965).

[39]R. F. Frosch, J. S. McCarthy, R. E. Rand, and M. R. Yearian, Phys. Rev. 160, 874 (1967).

[40]H. Frank, D. Haas, and H. Prange, Phys. Lett. 19, 391 (1965).

[41]L. I. Schiff, Phys. Rev. 133, B802 (1964).

[42]H. Collard, R. Hofstadter, E. B. Hughes, A. Johansson, M. R. Yearian, R. B. Day, and R. T. Wagner, Phys. Rev. 138, B57 (1965).

[43]If instead of using a hard-core potential to determine δ we use the nucleon-nucleon potential with which we performed the present scattering calculations, then the value $\delta = 0.022$ fm is obtained.